High-Risk (HPV16) Human Papillomavirus E7 Oncoprotein Is Highly Stable and Extended, with Conformational Transitions that Could Explain Its Multiple Cellular Binding Partners†

Leonardo G. Alonso,‡ Maria M. García-Alai,‡ Alejandro D. Nadra,‡ Alicia N. Lapeña,‡ Fabio L. Almeida,§ Peter Gualfetti,|| and Gonzalo de Prat-Gay*,†

Instituto Leloir, Facultad de Ciencias Exactas y Naturales, Universidad de Buenos Aires, Patricias Argentinas 435, (1405) Buenos Aires, Argentina, Genencor International, Inc., 925 Page Mill Road Palo Alto, California 94304, and Centro Nacional de Resonancia Magnetica Nuclear, Departamento de Bioquimica Medica, Universidade Federal do Rio de Janeiro, Rio de Janeiro 21941-590, Brazil

Received January 23, 2002; Revised Manuscript Received April 24, 2002

ABSTRACT: High-risk papillomaviruses are known to exert their transforming activity mainly through E7, one of their two oncoproteins. Despite its relevance, no structural information has been obtained that could explain the apparent broad binding specificity of E7. Recombinant E7 from HPV-16 purified to near homogeneity showed two species in gel filtration chromatography, one of these corresponding to a dimer with a molecular weight of 22 kDa, determined by multiangle light scattering. The E7 dimer was isolated for characterization and was shown to undergo a substantial conformational transition when changing from pH 7.0 to 5.0, with an increase in helical structure and increased solvent accessibility to hydrophobic surfaces. The protein was resistant to thermal denaturation even in the presence of SDS, and we show that persistent residual structure in the monomer is responsible for its reported anomalous electrophoretic behavior. The dimer also displays a nonglobular hydrodynamic volume based on gel filtration experiments and becomes more globular in the presence of 0.3 M guanidinium chloride, with hydrophobic surfaces becoming accessible to the solvent, as indicated by the large increase in ANS binding. At low protein concentration, dissociation of the globular E7 dimer was observed, preceding the cooperative unfolding of the structured and extended monomer. Although E7 bears properties that resemble natively unfolded polypeptides, its far-UV circular dichroism spectrum, cooperative unfolding, and exposure of ANS binding sites support a folded and extended, as opposed to disordered and fluctuating, conformation. The large increase in solvent accessibility to hydrophobic surfaces upon small pH decrease within physiological range and in mild denaturant concentrations suggests conformational properties that could have evolved to enable protein−protein recognition of the large number of cellular binding partners reported.

High-risk human papillomaviruses (HPVs) are directly linked to cervical carcinomas, a predominant disease among malignancies in women (*1*). HPV16 E7 and E6 proteins play key roles in the oncogenic process through their ability to interact with tumor suppressors retinoblastoma (RB) and p53, respectively (*2*). In particular, E7 is the major transforming activity, whereas E6 is more related to conferring malignancy. E7 is a 98 amino acid acidic protein (*3*) containing zinc (*4*, *5*) and is present in all papillomaviruses. It shares sequence and functional features with adenovirus E1A protein and SV40 T antigen (*6*), including the ability to disrupt the interaction between transcription factor E2F and the Rb protein, which releases transactivation competent E2F (*7*). Binding to Rb is essential for the transforming activity of high-risk HPVs (i.e, strains 16 and 18), since low-risk strains show little or no affinity for Rb (*8*).

Although the best described interaction of E7 with a cellular target is that with the Rb tumor suppressor (*9*), it can interact with a vast number of cellular proteins related to cell growth and transformation (*10*), gene transcription (*11*), apoptosis, and DNA synthesis, among other processes (*12*). A large number of different proteins were described to interact with E7, and these include glycolytic enzymes (*13*, *14*), histone deacetylase (*15*), kinase p33CDK2, and cyclin A (*16*). Despite the large body of functional information in

† This work was supported by a CRP Grant (Arg 98-02 r1 and r2) from the Institute for Genetic Engineering and Biotechnology (ICGEB-Trieste, Italy). G.P.G. wishes to acknowledge the support from Fundacion Antorchas and Fundación Bunge y Born. The work was supported in part by a Carrillo-Oñativia Fellowship from the Argentine Health Ministery. L.G.A. holds a fellowship from CONICET, A.D.N. was supported by a Carrillo-Oñativia Fellowship, and M.M.G.A. holds a studentship from the University of Buenos Aires.

* Corresponding author. E-mail: gpratgay@leloir.org.ar.

‡ Universidad de Buenos Aires.

§ Universidade Federal do Rio de Janeiro.

|| Genencor International, Inc.

[1] Abbreviations: $E7_2$, E7 dimer; MBP, maltose binding protein; IPTG, isopropyl-1-thio-b-D-galactopyranoside; SDS, sodium dodecyl sulfate; PAGE, polyacrylamide gel electrophoresis; DTT, dithiothreitol; ANS, 8-anilino, 1-naphthalene sulfonate; PAR, 4-(2-pyridylazo)-resorcinol; PMPS, p-hydroxymercuriphenylsulfonate; PMSF, phenylmethylsulfonylfluoride; GdmCl, guanidinium chloride; Tris, tris-(hydroxy-methyl)aminomethane; EDTA, ethylenediaminetetraacetic; LB, Luria-Bertani; kDa, kilodalton(s); CD, circular dichroism; Rb, tumor suppressors retinoblastoma protein.

10.1021/bi025579n CCC: $22.00
Published on Web 07/25/2002

vivo, there is still no structural information available to explain its apparent broad specificity and puzzling conformational properties. Functional HPV16 E7 recombinantly expressed in bacteria was shown to contain strongly bound tetrahedral zinc and displayed an apparently disordered far-UV circular dichroism spectrum (*17*). Only recently have the oligomerization properties of E7 started to be addressed by equilibrium sedimentation analysis, where monomers, dimers, and tetramers were detected (*18*).

In the present work, we isolated and characterized an E7 dimer and found that it displays an extended conformation with nonglobular behavior, with a thermoresistant E7 monomer. The E7 dimer is capable of undergoing structural transitions that generate hydrophobic surfaces accessible to solvent upon pH changes within a physiological range and in mild denaturant concentrations. We discuss our findings in connection with its properties regarding the ability of E7 to interact with a wide range of protein partners in the cell.

EXPERIMENTAL PROCEDURES

Expression and purification of HPV 16 E7. HPV 16 E7 was cloned as a thrombin cleavable fusion protein to the maltose binding protein (MBP) into a pMALp2 vector (New England Biolabs, Beverly, MA), a generous gift from Mark Bycroft, and expressed in *E.coli* TB1 strain. Cell cultures were grown in 5 L of LB medium at 37 °C containing 100 μg/mL of ampicilin. Four hours after inoculation, 0.4 mM IPTG was added to the culture for induction. Cells were harvested by centrifugation after 18 h from induction and stored at −70 °C. The pellet was resuspended in buffer A (50 mM Tris-HCl, pH 7.5, 0.15 M NaCl, 1.0 mM 2-mercaptoethanol), lysed by sonication, and centrifuged at 12 000 rpm. The resulting supernatant was precipitated by adding solid ammonium sulfate to 80% saturation. The precipitated protein was collected by centrifugation, resuspended, and dialyzed against buffer A. The soluble fraction was subjected to an amylose affinity column (New England Biolabs, Beverly, MA) equilibrated with buffer A. MBP−E7 protein was eluted with 15 mM maltose in the same buffer. The MBP−E7 fraction was dialyzed against buffer A. $CaCl_2$ and human thrombin (Sigma, St Louis, MO) were added to a final concentration of 2.5 mM and 0.33% (w/w), respectively, and incubated for 2 h at 37 °C. The reaction was stopped by adding 2.0 mM of PMSF. The protein was dialyzed overnight against 50 mM Tris-HCl, pH 7.5, 50 mM NaCl, and 1.0 mM 2-mercaptoethanol. As expected from its broad specificity, E7 tends to interact with a number of different proteins, and this complicates the separation. In addition, it binds too strongly to the anionic exchange matrix, which in combination with the number of conformers observed made us consider performing the anion exchange step in urea. We found that not only it separates better from other proteins, it yields an homogeneous sample. Solid urea was added to a final concentration of 8 M and the sample was incubated for 1h and loaded onto a Q-HyperD column (BioSepra, Villeneuve la Garenne, France) equilibrated with 50 mM Tris-HCl, pH 7.5, 50 mM NaCl, 1.0 mM 2-mercaptoethanol, in 6.0 M urea. After washing with 5 column volumes, bound protein was eluted with a 50−800 mM NaCl linear gradient in urea. The fractions containing the E7 protein were pooled, and DTT was added to a 10 mM final concentration. The refolding step was performed by dialyzing the fraction against 1mM DTT, 20 mM Tris-HCl, pH 7.5, overnight at 4 °C. The refolded protein was concentrated by ultrafiltration and subjected to gel filtration chromatography, Superdex 75 (Pharmacia Biotech, Uppsala, Sweden).

Determination of protein concentration and bound zinc. Protein concentration was determined by Bradford colorimetric assay and confirmed by quantitative amino acid analysis with nor-leucine as a standard. Bound zinc was determined by spectrophotometric measurement of the metallochromic indicator PAR (*19*). In brief, purified $E7_2$ was dialyzed against phosphate buffer at pH 7.0 without DTT and treated with Chellex 100, to remove soft bound metal. One milliliter of a 5 μM concentration of the Chellex-treated protein was incubated with 100 μM of PAR reagent and 100 μM of PMPS in 0.1 M of sodium phosphate buffer pH 7.0. The reaction was followed at 500 nm and the amount of zinc quantified against a curve with a standard solution (Sigma, St Louis, MO). $E7_2$ was found to contain 1.15 mol Zn per mol of monomer. This corresponds, within experimental error, to a 1:1 stoichiometry, and we assume this throughout the work.

Gel electrophoresis and size exclusion chromatography. All experiments were performed according to the Laemmli method (*20*), except urea−SDS−PAGE experiments that were carried out using a Tricine−SDS−PAGE system (*21*). In brief, each sample was heated with sample buffer (0.125M Tris-HCl, 4% SDS, 6.0M urea, 0.02% bromophenol blue, 5.0mM EDTA, pH 6.8), resolved in a 12.5% acrylamide gel, and stained by coomassie blue.

Unfolding gel filtration experiments were carried out on a Superdex 75 equilibrated with 10 mM Sodium phosphate buffer pH 7.0, with 1.0 mM DTT and the indicated GdmCl concentration. The samples were incubated for 1 h before injection, and the elution of the protein was monitored at 276 nm. The column was calibrated with the following standard globular proteins: BSA (67 kDa), ovalbumin (43 kDa), chymotrypsinogen A (25 kDa), ribonuclease A (13.4 kDa) from a gel calibration kit (Pharmacia Biotech, Uppsala, Sweden). The void volume (V_0) and total volume (V_t) were determined by loading Blue Dextran and acetone, respectively, at each GdmCl concentration to check for column compression. All experiments were carried out at 25 °C unless indicated.

Circular Dichroism and Fluorescence Spectroscopy. CD measurements were carried out on a Jasco J-810 spectropolarimeter (Jasco, Japan) employing a scan speed of 20 nm/min, a band-pass of 1 nm, and an average response time of 4 s. All spectra were an average of at least10 scans. The temperature was kept at 25 °C using a Peltier temperature-controlled sample compartment. Spectra of $E7_2$ HPV 16 at 10 and 1.5 μM were taken on a 0.1 and 1.0 cm path length cells, respectively. Each point in the GdmCl unfolding experiments were incubated for 4 h in 10 mM sodium phosphate buffer, 1.0 mM DTT, pH 7.0 prior to measurement. For pH dependence experiments, 10 μM of purified $E7_2$ in 20 mM of sodium formiate (pH 2.5, 3.0, 3.5, 4.0); sodium acetate (pH 4.5, 5.0, 5.5, 6.0) or Tris-HCl (pH 7.5) buffers were used. Temperature denaturation curves of $E7_2$ were carried out in phosphate buffer pH 7.0 and monitored following the amplitude of negative ellipticity band at 220 nm.

Fluorescence emission spectra for ANS binding were carried out at 25 °C on a Aminco-Bowman spectrofluorimeter with excitation at 350 nm, 4 nm band-pass, and processing an average of two spectra. $E7_2$ was kept at 10 μM in each condition, and ANS concentration was 100 μM, determined from saturation experiments (not shown).

NMR spectra. 1D 1H NMR spectra were acquired in a Bruker DRX 600 MHz. $E7_2$ at 250 μM was resuspended in 50 mM phosphate buffer, pH 7.1 and 5.0 mM DTT. The spectra were recorded after 4 h incubation at 25 °C.

Multiangle Laser Light Scattering. Multiangle laser light scattering data were collected on a DANM DSP laser photometer emitting light at 633 nm and detecting at 18 fixed angle positions around a K5 flow cell (Wyatt Technologies, Santa Barbara CA). Protein concentration was determined by an OPTILAB DSP interferometric refractometer (Wyatt Technologies). Molecular weight calculations were performed on the ASTRA 4.73 software supplied with the instrument. E7 was run in 10 mM Tris-HCl at pH 7.5 with 1.0mM DTT over a preequilibrated TSK-GEL G3000SWXL size exclusion chromatography column (TosoHaas) at 25 °C prior to collection of light-scattering data. Data were also collected in the same buffer with the addition of 0.3M GdmCl. The protein concentration was ~100 μM in all experiments.

RESULTS

Isolation of a stable HPV16 E7 dimer. HPV16 E7 was purified from a maltose-binding protein fusion and an unfolding/refolding step, to near homogeneity as judged by SDS−PAGE (Figure 1a, inset). As explained in the Experimental Section, the use of urea yields a more conformationally homogeneous sample and largely improves the separation. Strongly cystein bound zinc is present right from the early folding steps in the cytosol; therefore, the urea unfolded E7 already contains the strongly bound metal. When refolding from urea unfolded E7 was carried out by dialysis in the presence of added zinc at pH 7.5, two species of 60 and 46 kDa were found on a Superdex 75 gel filtration column (Figure 1a). These two species are not in equilibrium, after at least 2 h incubation prior to reinjection (not shown). Refolding urea unfolded E7 in the absence of added zinc in the dialysis buffer in combination with a shock treatment with 10mM DTT prior to dialysis causes the 60 kDa species (Figure 1a, peak I) to virtually disappear. The peak corresponding to a globular 46 kDa protein (peak II) can be separated by gel filtration and always contain 1 mol of strongly bound zinc per mol of monomer, irrespective of how the species was obtained. The 60 kDa running species does not involve the formation of a disulfide bridge since SDS−PAGE of the peaks give a single band irrespective of the presence or absence of reductant (Figure 1b).

A multiangle light-scattering experiment (see experimental procedures) yields a molecular mass of 22 kDa for the 46 kDa running species, confirming the equilibrium sedimentation data (*18*), but now analyzed with a direct measurement on the isolated species. The expected molecular weight of the monomer is ~11 kDa but displays an anomalous electrophoretic behavior, explained below. Using the PAR colorimetric assay for bound zinc (*19*), we measured 1 mol of zinc per mole of E7 monomer in the E7 dimer (see

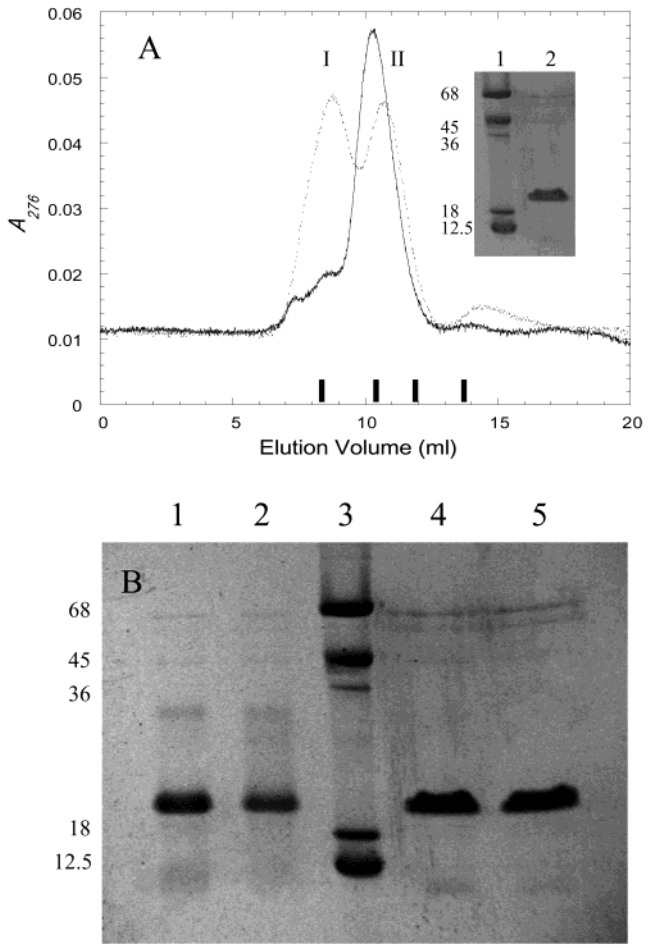

FIGURE 1: Different species after purification of E7 to homogeneity. (A) Size exclusion chromatography of purified E7 in a Superdex 75 column following refolding with (dotted line) or without (full line) addition of zinc. For refolding, purified E7 was incubated at 60 μM with 8 M of urea and was dialyzed against 20 mM Tris-HCl pH 7.5, 1.0 mM 2-mercaptoethanol plus the addition of 100 μM of $ZnSO_4$ or without added zinc in the dialysis buffer in combination with a shock treatment with 10 mM DTT prior to dialysis. The four vertical bars denote the positions of molecular size standards, from left to right: BSA (67 kDa), ovalbumin (43 kDa), chymotrypsinogen A (25 kDa), ribonucleaseA (13.4 kDa). Inset: purified recombinant E7. 12.5% SDS−PAGE stained with Coomassie Brilliant Blue R-250. Lane 1, molecular weight marker in kDa. Lane 2, E7. (B) Effect of DTT on isolated peaks from size exclusion chromatography. Samples isolated from the size exclusion chromatography that eluted at a volume corresponding to a globular protein of ~60 kDa (peak I) and ~46 kDa (peak II), assuming that globular conformations (peak II) were treated with sample buffer, incubated for 10 min at 95 °C, in the presence or absence of 10 mM DTT when indicated. Coomassie blue stained SDS−PAGE 12.5%. Lane 1 and 2, peaks I and II, respectively, without DTT; lanes 3, molecular weight markers; lanes 4 and 5, peaks I and II, respectively, plus DTT.

experimental procedures), strongly suggesting that the tetrahedrically cystein coordinated zinc was formed at the initial folding events in the bacterial cytosol. If we add EDTA and reductant to urea unfolded E7, the protein cannot refold properly, and high-molecular-weight aggregates are formed, eluting in the exclusion volume of the gel filtration column. These results suggest that the conversion into the larger 60 kDa running species may involve soft bound zinc, which is eliminated by the excess of DTT, acting as metal scavenger rather than a reductant. The sole addition of 0.1 mM zinc to 46 kDa $E7_2$ does not produce any of the 60 kDa running

species, and addition of 0.5 mM zinc leads to aggregation (not shown). Formation of the 60 kDa species can only take place if the protein is unfolded in urea and the 0.1 mM zinc added in the refolding buffer, in the absence of DTT.

pH induces a structural transition in E7. The far-UV CD spectrum of $E7_2$ at pH 7.5 is dominated by a minimum at 205 nm, with a band at around 220 nm and a small but clear maximum at around 190 nm (Figure 2a). The band at 220 nm is indicative of α-helix content, and the minimum at 205 can be interpreted as a mixture of α-helix (208 and 220 nm) and disordered structure (200 nm). As the pH of the buffer is lowered, the ellipticity at 220 nm decreases, suggesting an increase in helical content (Figure 2a). The protein aggregates around pH 4.5 approximately at its pI (spectra not shown), and below pH 3.5 it becomes less structured but with an evident α-helix nature. The spectra at pH 5.0 shows the typical features of α-helix, i.e., minima at 208 and 222 nm, and a maximum at 192 nm, while at pH 2.5 the helical features are present, albeit with less intensity (Figure 2a). Upon returning to pH 7.5, the spectrum is fully recovered, and therefore, we assume full reversibility (not shown). Figure 2b shows the ellipticity change at 220 nm against pH.

An increase in the accessibility of hydrophobic regions to solvent in the species at pH 5.0 can be inferred from the large increase in the ANS binding (Figure 2c). This would indicate that a substantial conformational change that takes place on pH decrease within a physiological range not only occurs at the level of the secondary structure but also on tertiary structure, and the newly solvent-accessible hydrophobic surfaces must necessarily provide binding properties that will be rather different to those at pH 7.0. The structural transition displays an apparent pK_a of around 6.0, which can either be ascribed to histidine residues or acid groups with anomalous pK_a. Such was the case described for peptides containing polyglutamic acid (*22*). The transition below the pI simply indicates loss of structure due to acid denaturation.

Resistance of $E7_2$ to thermal denaturation in the presence of SDS. As previously reported, E7 behaves as a 19 kDa polypeptide on SDS−PAGE even though its molecular weight approaches 11 kDa (*17*, *23*). This was ascribed to charge effects on the electrophoretic behavior based on mutation of asp4 for arginine which recovered the expected behavior (*24*). On the basis of preliminary experiments that show that E7 was thermostable, our hypothesis was that the anomalous electrophoretic behavior could be due to residual structure, altered by the drastic replacement of an aspartic residue for an arginine. The far-UV CD spectrum of $E7_2$ at 90 °C and in the presence of SDS shows that not only is it not denatured, it also appears to become more structured, as judged by the shift and increase in both α-helix indicative bands (208 and 222 nm) (Figure 3a).

To test the hypothesis that the anomalous behavior is due to a stable and extended structure, we carried out an SDS−PAGE experiment either in the absence or presence of 8 M urea in the gel. Adding 8 M urea to both cracking buffer and gel causes E7 to run as a 14 kDa polypeptide, instead of 19 kDa, in the absence of urea (Figure 3b). If urea is added only to the cracking buffer but not to the separating gel, the electrophoretic mobility remains as 19 kDa, suggesting that the presumably extended structure of E7 is quite stable and tends to refold fast in the absence of the denaturant in the gel. The fact that the mobility is not completely as expected even with 8 M urea (11kDa), together with the smear in the band, indicative of conformational equilibrium, adds further evidence of the high stability of the structure responsible for the anomalous electrophoretic behavior.

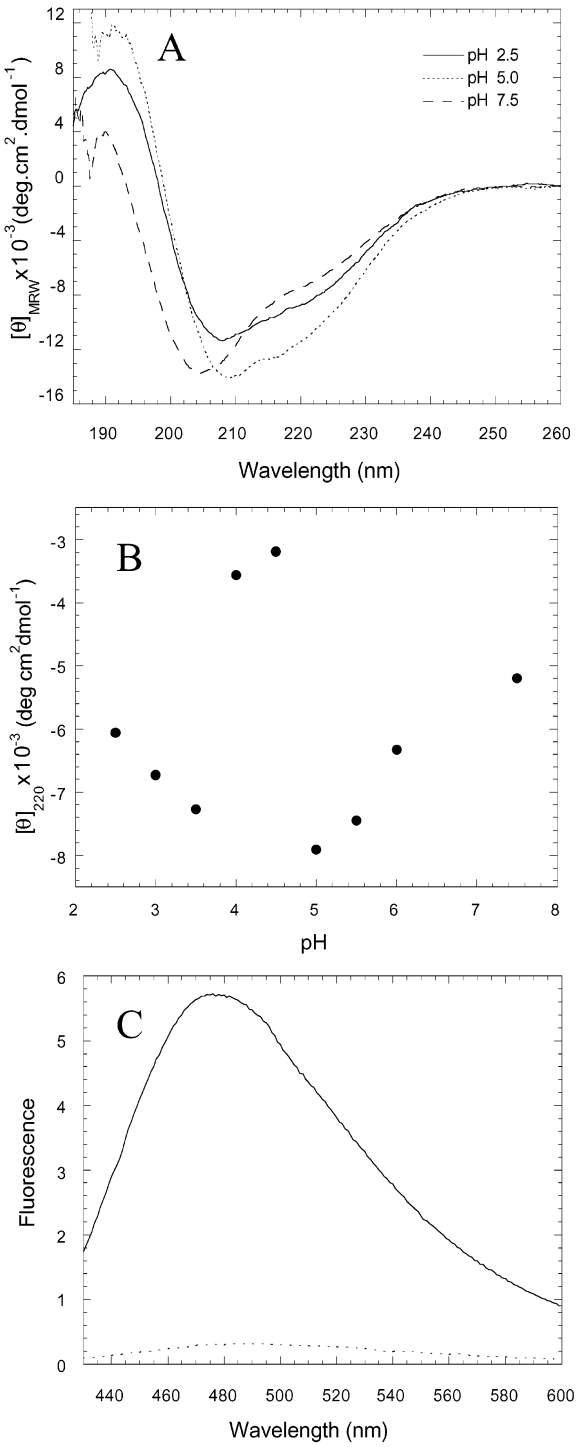

FIGURE 2: Conformational changes in the $E7_2$ dimer induced by pH. (A) Circular dichroism spectrum of $E7_2$ at different pH (see Experimental Procedures). (B) Molar ellipticity of $E7_2$ at 220 nm as function of pH. The data at pH 4.0 and 4.5 showed turbidity, indicating aggregation as expected around the theoretical isoelectric point (pI 3.9). C) ANS binding to $E7_2$ as function of pH. Fluorescence emission spectrum of 100 μM ANS in the presence of 10 μM $E7_2$ in 20 mM of Tris-HCl pH 7.5 (dotted line) and 20 mM of sodium acetate buffer pH 5.2 (full line); all samples were incubated at 25 °C for 1 h prior to measurement. The contribution of free ANS at 100 μM at each pH was subtracted.

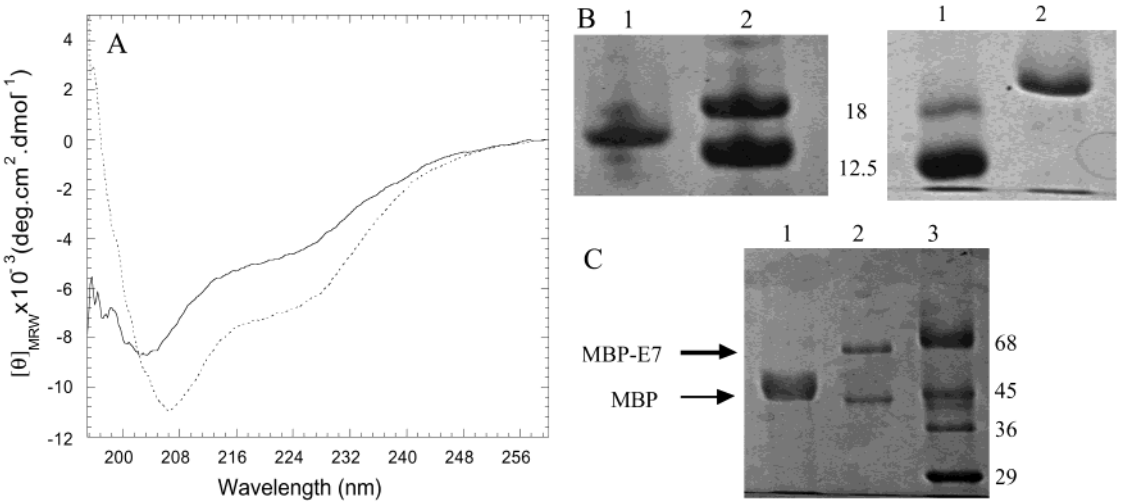

FIGURE 3: Resistance to heat SDS denaturation as the basis for the anomalous electrophoretic behavior of $E7_2$. (A) Circular dichroism spectrum of $E7_2$ at 90 °C (full line) and at 90 °C plus 20 mM SDS (dotted line) in 10 mM of sodium phosphate buffer, pH 7.0. The samples were incubated for 10 min before measurement. (B) Left panel: 12.5% urea−SDS−PAGE of purified E7 stained with coomassie blue (see Experimental Procedures). Lane 1, E7; lane 2, molecular weight markers in kDa. Right panel: 12.5% SDS−PAGE. Lane 1, molecular weight markers; lane 2, E7. All samples were treated according to experimental procedures prior to running. (C) Ruling out dimerization of the MBP-E7. The fusion protein was partially cleaved with thrombin and analyzed in 10% SDS−PAGE. Lane 1, MBP (∼45 kDa) after full cleavage of MBP-E7 fusion protein; lane 2, partially cleaved MBP-E7 fusion protein(∼64 kDa); lane 3, markers.

The next question is whether the 19 kDa SDS−PAGE running species is effectively a hyperstable dimer ($E7_2$) or an extended monomer. To test this, we made use of the MBP-E7 fusion protein; if E7 runs as a dimer in SDS−PAGE, then the MBP-E7 fusion should run as double the size of MBP plus E7 (the hypothetical 19 kDa running dimer). MBP-E7 was partially digested with thrombin and analyzed by SDS−PAGE. Cleaved MBP expectedly runs as a 45 kDa polypeptide, and the fusion runs exactly as 45 plus 19 kDa, corresponding to extended E7 (Figure 3c). If E7 remained as a dimer, the fusion should stay as a dimer as well, and the expected migration would be equivalent to 109 kDa (2-fold the molecular weight of the E7-MBP fusion). In any case, the fusion protein runs as ∼64 kDa from the expression follow-up and throughout the purification steps.

Globularization and dissociation of $E7_2$ precede unfolding of the E7 monomer by GdmCl. Having isolated a defined dimeric species of E7, we further characterized it by unfolding using chemical denaturants. Guanidinium chloride denaturation experiments were monitored in parallel by circular dichroism and size exclusion chromatography. In both cases there is a biphasic response with a first transition at 0.3 M GdmCl concentration (Figure 4a,b). The far UV−CD spectrum indicates that the increase of negative ellipticity corresponds to an increase in structure (Figure 4c). Light-scattering measurements yield a molecular weight of 22 kDa for the species at 0.3 M GdmCl, indicating that $E7_2$ does not undergo dissociation in these conditions. Thus, our interpretation is that the E7 dimer becomes more compact with a more globular-like behavior. At 10 μM protein concentration, from 0.3 M denaturant onward, both molar ellipticity and elution volume transitions take place in parallel (Figure 4b). The complete transition from 0.3 to 6.5 M GdmCl involves a molar ellipticity change of 6800 deg dmol^{-1} cm^2 and a 2.0 mL change in the elution volume, both compatible with the unfolding of a globular protein. There is no evidence of residual structure at 6.5 M GdmCl, as judged by the far-UV CD spectrum (Figure 4c). We carried out a GdmCl denaturation experiment at a lower protein concentration (1.5 μM), and the transition is represented in Figure 5a. The same biphasic behavior is observed, i.e., increase in negative ellipticity from 0 to 0.3 M GdmCl and subsequent decrease, indicative of loss of structure. However, there are two transitions that become more evident in the experiment at lower protein concentration, one from 0.3 to 2.0 M GdmCl and the other from 2.0 to 6.5 M denaturant. The displacement of the first transition at lower protein concentration strongly suggests that this phase involves dissociation of the dimer. In the second transition, both experiments are superimposable, strongly suggesting the unfolding of the E7 monomer, where the 6.5 M GdmCl species is the unfolded E7 monomer.

To evaluate the stability of the different species in the transition, we carried out a thermal denaturation monitored by changes in molar ellipticity. In the absence of denaturant there, is no significant change in ellipticity (Figure 5b), which confirms a high thermal stability, in agreement with the spectra obtained at 90 °C and SDS (Figure 3a). To our surprise, at 2.5 M GdmCl concentration, the protein still does not denature by temperature (Figure 5b). There is a small ellipticity change when the species at 0.3 M GdmCl was subjected to thermal denaturation, which we interpret as dissociation since the final ellipticiy is coincident with the end of the dissociation transition in the GdmCl renaturation (see discussion).

Figure 6 shows the aromatic and amide region of the one-dimensional 1H NMR spectra in 0, 0.3, and 0.7 M GdmCl. In all conditions tested, E7 shows low chemical shift dispersion. The addition of denaturant to 0.3 and 0.7 M GdmCl does not lead to greater chemical shift dispersion. This could be explained by the small change in ellipticity observed. As the GdmCl concentration is increased, the lines become sharper, and at 0.7 M, they become better resolved. Changes in peak broadening can be analyzed by looking at well-resolved lines, such as the resonances between 7 and 7.1 ppm (Figure 6, arrows). The globularization observed at

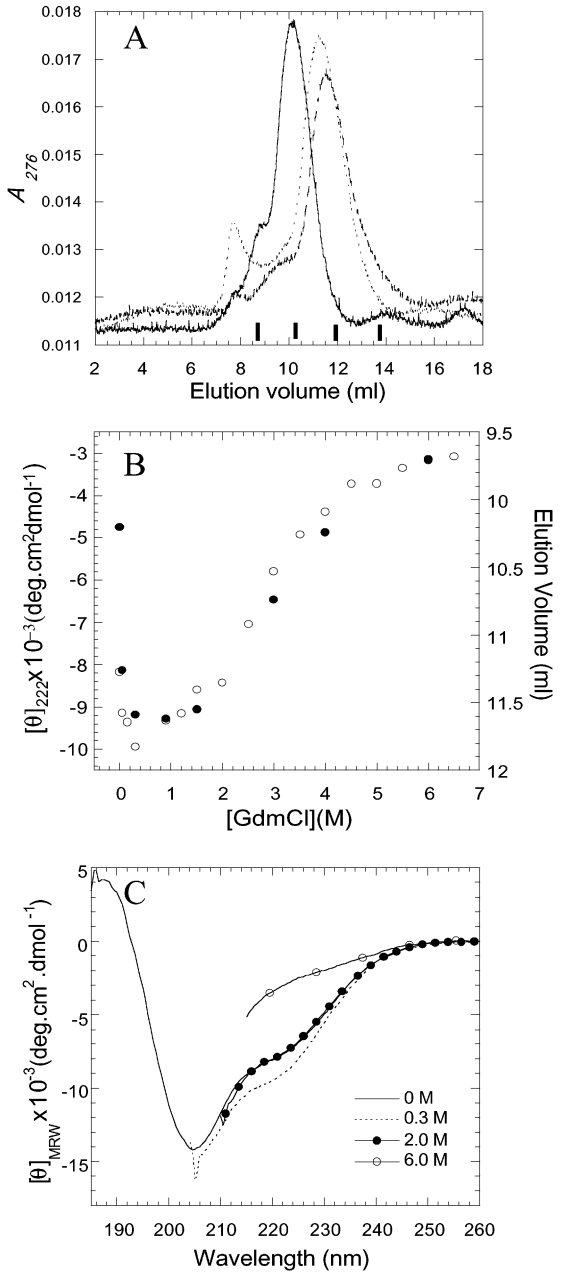

FIGURE 4: Globularization, dissociation and unfolding of $E7_2$ by guanidinium chloride. (A) Size exclusion chromatography of E7 was carried out on a Superdex 75 column at different GdmCl concentrations. Full line, 0 M GdmCl; dashed line, 0.3 M GdmCl; dotted line, 1.5 M GdmCl. The column was equilibrated with the indicated denaturant concentration in 10 mM sodium phosphate buffer pH 7.0, 1.0 mM DTT. Samples were incubated for 4 h at each GdmCl concentration before running. The four vertical bars denote the positions of molecular size standards, from left to right: BSA (67 kDa), ovalbumin (43 kDa), chymotrypsinogen A (25 kDa), ribonucleaseA (13.4 kDa). B) Guanidinium chloride-induced unfolding of E7 protein monitored in parallel by changes in far-UV CD at 220 nm and size exclusion chromatography. Open circles, molar ellipticity at 220 nm; solid circles, elution volume (mL, inverted scale). (C) Circular dichroism spectrum of E7 at different GdmCl concentrations.

0.3 M GdmCl appears to increase the resolution of bands; however, this seems to be further improved at 0.7 M GdmCl. We believe that the transition to the compacted conformation observed at 0.3 M is not complete and 0.7 M chaotrope is required. The unfolding of the monomer begins to take place only after 1.5 M GdmCl (Figure 5a).

The different stages of the unfolding transition were further characterized by monitoring the ability to bind ANS. At pH 7.5 in the absence of denaturant, $E7_2$ binds only a fraction of the hydrophobic dye, as the small increase in fluorescence suggests, to the same extent as the species at 2.0 M GdmCl, presumably a partly folded monomer (Figure 7). The compacted dimeric species at 0.3 M GdmCl shows a dramatic increase in ANS binding, with a maximum at ~480 nm, while at 6.5 M GdmCl there is no ANS binding as expected for an unfolded polypeptide. On the basis of studies of ANS binding sites, the λ_{max} is indicative of the polarity of the site (*25*); a polar site can go up to 497 nm (*26*). Therefore, it is reasonable to assume a somehow hydrophobic nature for the newly formed accessible ANS site in E7.

DISCUSSION

E7 plays a key role in the transformation of epithelia in papillomavirus related cancers. Although the best described cellular target is the Rb tumor suppressor, a vast number of different cellular proteins were reported to interact with E7 (*27*). It is hard to envision how a single small protein can display such a wide range of specific interactions. Nevertheless, this broad specificity must necessarily be related to distinctive structural and conformational properties. Despite its relevance, there is no structural information available for E7; yet it can be expressed recombinantly (*17*, *28*, *29*) and is highly soluble. Our effort has been directed to the understanding of its conformational properties in solution, hopefully clearing the way for detailed structural studies.

E7 purified to near homogeneity elutes as 46 and 60 kDa globular molecular weight species in a gel filtration column. SDS−PAGE experiments show that there is no intermolecular disulfide formation, and the two peaks run as the same single band. We found that these species are not interconvertible within several hours and the 60 kDa eluting species can only be obtained by treatment with 8 M urea and subsequent dialysis in the presence of added zinc, but not by simply adding zinc to $E7_2$ once it is folded, suggesting an energy barrier between the two species requiring at least partial unfolding or rearrangement of the dimer. The zinc molecules participating in the formation of the 60 kDa eluting species must be other than strong tetrahedrically coordinated zinc, since treatment with DTT can enrich the dimeric species, most likely by scavenging softly bound zinc atoms (*29*). On the basis of far UV CD spectra, it was previously suggested that addition of cadmium could replace the strongly cystein bound zinc (*17*). We found that spectral changes do take place after the addition of excess zinc or cadmium, but these are the effect of aggregation, presumably through soft metal binding sites that that are formed intermolecularly (not shown). Multiangle light-scattering experiments presented here indicate that the isolated 46 kDa eluting species is a dimer, a direct measurement that agrees with what was found in equilibrium sedimentation analysis (*18*).

Upon decreasing the pH from 7.5 to 5.0, the E7 dimer undergoes a marked conformational transition, where an increased helical content is observed. The protein aggregates between pH 4.5 and 4.0, around its pI and shows substantial helical content at pH 3.6, disappearing as the pH is further decreased. The species at pH 5.0 shows an incremented

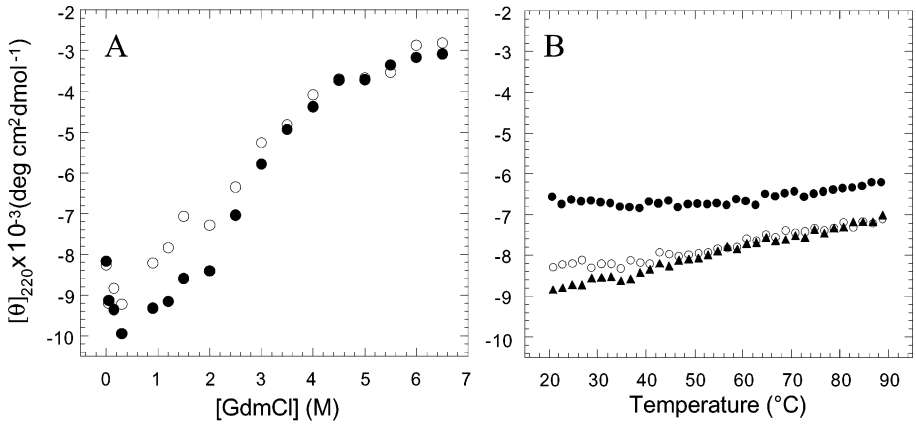

FIGURE 5: Dependence of E7 GdmCl denaturation on protein concentration and thermal stability of the different species. (A) Molar ellipticity at 220 nm of E7 at 10 μM, solid circles and at 1.5 μM, open circles, as function of GdmCl concentration (see experimental procedures). (B) Thermal denaturation of 10 μM $E7_2$ monitored by changes in molar ellipticity at 220 nm. Open circles, 0 M GdmCl; closed triangles, 0.3 M GdmCl; closed circles, 2.5 M GdmCl.

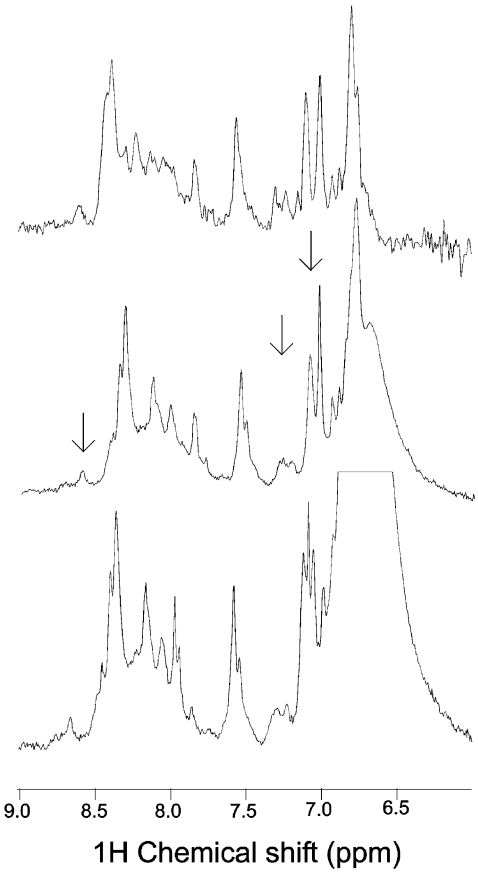

FIGURE 6: Amide and aromatic region of 1D proton spectra of $E7_2$ at different guanidine chloride concentrations. The spectra were obtained in a Bruker DRX 600 at 398 K. GdmCl was added, and the 1D proton spectra were obtained after 2 h. Top, 0 M, middle, 0.3 M, and bottom, 0.7M GdmCl. Arrows indicate some isolated peaks that resolve better as the denaturant increases.

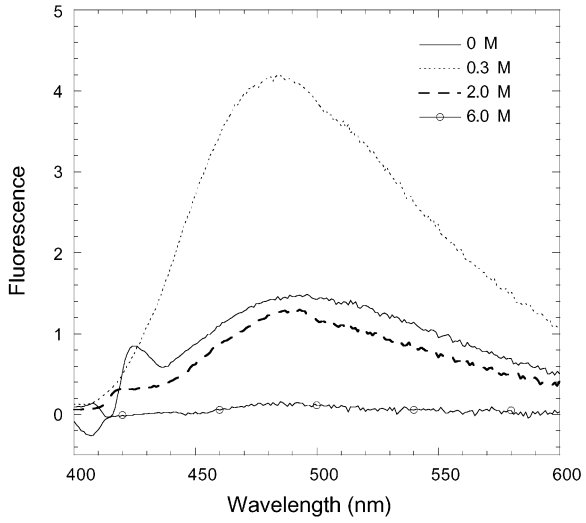

FIGURE 7: ANS binding of E7 after the GdmCl-induced conformational transition at the diferent denaturant concentrations indicated.

capacity to bind ANS, suggesting the formation of solvent accessible hydrophobic sites. Thus, a substantial conformational change takes place within a physiological range of pH that causes the protein to expose new regions to the solvent. Considering the broad range of proposed cellular partners for E7, one can speculate that subtle changes in cell pH, or in any of its compartments, can have a dramatic effect on the type of target proteins with which E7 interacts within the cell. The cell nucleus is populated with histones and other basic proteins, some of which are potential targets of E7, including cellular transcription regulators. In this context, the conformation or oligomerization state of the oncoprotein will be largely dependent on the microenvironment where the transcription related processes take place allowing for at least some recognition selectivity. For example, the nuclear and cytoplasmic environment is likely to change along the differentiation process of the HPV infected epithelia, going from basal cells to highly differentiated queratinocytes.

The well-known anomalous electrophoretic mobility of E7 in SDS−PAGE (*24*) was shown to be normalized by mutation of asp4 to arginine. This rather drastic mutation is otherwise based on sequence homology with low-risk HPV strains (*23*). Sequence comparison of the most relevant strains show that aspartic or glutamic residues are present in strain-16 and a few other strains. The rest of the strains alternate among either arginine, lysine, and asparagine, and several display a proline residue, including the high-risk HPV-18. This position could be key in the determination of stability, and this could not only influence its structure but its hydrodynamic properties.

The anomalous electrophoretic behavior can be explained by persistent structure, since it was shown to be resistant to

the combined effects of high temperature and SDS, and its expected mobility was largely restored when urea was added. However, the residual structure causes it to behave as an extended rather than a more compact molecule. When urea was used in the cracking buffer but not in the gel, the protein still behaved anomalously, suggesting that the stable and extended structure is recovered rapidly upon reduction of the temperature and dilution of the urea. In a gel filtration experiment, the E7 monomer in urea would run as an unfolded 11 kDa protein, with a larger hydrodynamic radius. This can be observed in the GdmCl experiment (Figure 4B) where the unfolded monomer behaves as a ~50 kDa globular protein, a volume increase expected for the unfolding of any globular or nonglobular protein. The folded monomer in principle is populated at 2.5 M GdmCl (Figure 5A), behaving as a ~32 kDa globular protein. Therefore, if a folded monomer could be isolated, this would be extended too.

Although the mutation of asp4 to arginine confers the expected electrophoretic mobility, our results suggests that this could be explained by the effect of this mutation on the extended conformation of E7, persistent under SDS−PAGE conditions. A previous functional mapping performing several three amino acid deletions at the N-terminal domain (*30*) did not produce a normal electrophoretic behavior, stressing that it is not merely a charge effect.

That the 19 kDa running species is not a denaturation resistant dimer was confirmed by experiments with the E7-MBP fusion, which leads us to conclude that the 11 kDa E7 monomer retains a extended structure in SDS−PAGE that causes it to behave as a 19 kDa polypeptide. In line with this is the anomalous hydrodynamic volume of the E7 dimer, which behaves as a ~46 kDa globular protein but was measured to be 22 kDa by light scattering experiments. Taken together, these results indicate that $E7_2$ bears an extended conformation, a property that is retained in the E7 monomer, where the latter showed to be thermoresistant.

Low concentrations of GdmCl give rise to a conformational change in $E7_2$ to a state with increased helical content and a very large change in hydrodynamic volume. The species at 0.3 M GdmCl elutes as a ~28 kDa protein, and its dimeric nature was confirmed by light scattering measurements. Thus, under these conditions, a globular conformation of $E7_2$ is induced, as opposed to its extended native conformation. Despite its highly stable structure, preliminary NMR spectra show that there is little chemical shift dispersion, which, in the absence of the body of experimental data we have gathered, would be interpreted as a disordered polypeptide. In agreement with the information from CD, extended structures tend to display little chemical shift dispersion (*31*). This extended conformation is clearly stabilized by the repulsion between the large number of negatively charged residues concentrated at the N-terminal half of the molecule. Protonation of key charged residues upon pH reduction or charge screening by 0.3 M GdmCl shifts the equilibrium toward α-helix, resulting in a more compact dimer with a large increase in solvent accessible hydrophobic surfaces, indicated by the increased ANS binding in both species. In any case, their CD spectra are different, and the form at pH 5.0 appears to have increased helical content.

From 0.3 to 2.0 M GdmCl approximately, the transition corresponds to dissociation of $E7_2$, clearly differentiable at

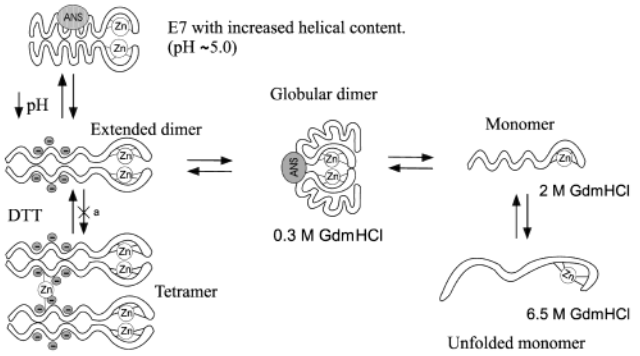

FIGURE 8: Proposed conformational transitions in HPV-16 E7.

1.5 μM as opposed to 10 μM protein concentration. The transition between 2.0 and 6.5 M is coincident at both protein concentrations, strongly suggesting that it corresponds to the unfolding of the E7 monomer. At 6.5 M GdmCl, E7 is devoided of observable secondary structure, but its hydrodynamic volume is only slightly larger than that of $E7_2$ in the absence of denaturant.

The results presented here can be summarized in Figure 8. We have isolated the E7 dimer, which appears to be the most representative conformation in our experimental conditions. However, it remains to be established which is the predominant form in the cell. The fairly weak dissociation constant (*18*) suggests that both monomer and dimer could be active in vivo, but an estimation of the concentration of E7 in the cell becomes essential. The dimer (i) always contain one strongly cystein coordinated zinc atom per monomer, (ii) has a nonglobular, extended conformation, (iii) undergoes a marked conformational pH transition within a physiological range, involving the exposure of hydrophobic patches, (iv) can form a higher order structure, possibly a tetramer, if zinc is included in the refolding, (v) forms a compact, globular dimer at 0.3 M GdmCl with increased solvent accessibility to hydrophobic sites, and (vi) dissociates to a stable extended monomer with substantial amount of structure that unfolds at high concentrations of denaturant. The putative tetramer is not in equilibrium with the dimer and an energetic barrier must be overcome for it to accumulate. In previous studies, the gel filtration matrix used did not allow the separation of these two species prior to the equilibrium sedimentation analysis (*18*). The fact that the dimeric and monomeric species are in equilibrium with a dissociation constant in the micromolar range does not favor the possibility that E7 could dimerize by the zinc atoms (*5*), and therefore, the metal must be coordinated tetrahedrically within the monomeric polypeptide.

Natively unfolded proteins are so defined by the lack of ordered structure under conditions of neutral pH in vitro (*32*, *33*). A recent survey based on amino acid sequence analysis showed that they display a low overall hydrophobicity and a large net charge as the major structural feature in common (*34*). E7 shares not only these features with natively unfolded polypeptides, but also the apparently disordered NMR spectra, its extended conformation, and the thermal stability. In fact, it was included in a list of natively unfolded polypeptides "ordered" by reversible cation binding (*34*). However, in E7, zinc atom is constitutive and it is strongly bound (*29*). In addition, we have shown a number of features that differentiates E7 from the average natively unfolded

polypeptide. Among these are a far-UV CD spectrum indicative of significative secondary structure, the capacity to form a structured dimer, a cooperative unfolding transition, and the capacity to bind ANS. We should add the possibility of E7 to be expressed recombinantly as an unfused polypeptide in bacteria without being degraded (*28*). E7 appears to represent an intermediate situation between extended disordered polypeptides and compact globular proteins. Nevertheless, all its features, including those in common with natively unfolded polypeptides, are clearly optimized for protein−protein interactions (*32*).

The possibility of isolating a homogeneous dimeric species of E7 will lead to improved conditions for structural studies both by crystallography and NMR. Eventual structural information, together with a deeper understanding of the peculiar conformational transitions of E7 described here, will hopefully lead to the dissection of the molecular mechanism behind the apparent broad specificity of this oncoprotein. The ability to expose hydrophobic surfaces upon a decrease in pH and globularization by mild denaturant conditions are likely to play a key role in its ability to interfere in many different cellular processes, some of which lead to malignant transformation.

ACKNOWLEDGMENT

We thank L. Banks for helpful criticisms to the manuscript.

REFERENCES

1. zur Hausen, H. (1996) *Biochim. Biophys. Acta 1288*, 55−78.
2. Tommasino, M., and Crawford, L. (1995) *Bioassays 17*, 509−518.
3. Cole, S. T., and Danos, O. (1987) *J. Mol. Biol. 93*, 599−608.
4. Barbosa, M. S., Lowy, D. R., and Schiller, J. T. (1989) *J. Virol. 63*, 1404−1407.
5. McIntyre, M. C., Frattini, M. G., Grossman, S. R., and Laimins, L. A. (1993) *J. Virol. 67*, 3142−3150.
6. Phelps, W. C., Yee, C. L., Munger, K., and Howley, P. M. (1988) *Cell 53*, 539−547.
7. Chellappan, S., Kraus, V. B., Kroger, B., Munger, K., Howley, P. M., Phelps, W. C., and Nevins, J. R. (1992) *Proc. Natl. Acad. Sci. U. S. A. 89*, 4549−4553.
8. Munger, K., Werness, B. A., Dyson, N., Phelps, W. C., Harlow, E., and Howley, P. M. (1989) *EMBO. J. 8*, 4099−4105.
9. Dyson, N., Howley, P. M., Munger, K., and Harlow, E. (1989) *Science 243*, 934−937.
10. McIntyre, M. C., Ruesch, M. N., and Laimins, L. A. (1996) *Virology 215*, 73−82.
11. Massimi, P., and Banks, L. (1997) *Virology 227*, 255−259.
12. Munger, K., and Halpern, A. L. (1995) in *HPV Sequence Database*, pp III-58−III-73, Los Alamos National Laboratory, Los Alamos, NM.
13. Zwerschke, W., Mazurek, S., Massimi, P., Banks, L., Eigenbrodt, E., and Jansen-Durr, P. (1999) *Proc. Natl. Acad. Sci. U.S.A. 96*, 1291−1296.
14. Mazurek, S., Zwerschke, W., Jansen-Durr, P., and Eigenbrodt, E. (2001) *Biochem. J. 356*, 247−256.
15. Brehm, A., Nielsen, S. J., Miska, E. A., McCance, D. J., Reid, J. L., Bannister, A. J., and Kouzarides, T. (1999) *EMBO. J. 18*, 2449−2458.
16. Tommasino, M., Adamczewski, P. J., Carlotti, F., Barth, C. F., Manetti, R., Contorni, M., Cavalieri, F., Hunt, T., and Crawdford, L. (1993) *Oncogene 8*, 195−202.
17. Pahel, G., Aulabaugh, A., Short, S. A., Barnes, J. A., Painter, G. R., Ray, P., and Phelps, W. C. (1993) *J. Biol. Chem. 268*, 26018−26025.
18. Clements, A., Johnston, K., Mazzarelli, J. M., Ricciardi, R. P., and Marmorstein, R. (2000) *Biochemistry 39*, 16033−16045.
19. Hunt, J. B., Neece, S. H., and Ginsburg, A. (1985) *Anal. Biochem. 146*, 150−157.
20. Laemmli, U. K. (1970) *Nature 227*, 680−685.
21. Schagger, H., and Von Jagow, G. (1987) *Anal. Biochem. 166*, 368−379.
22. Jelesarov, I., Durr, E., Thomas, R. M., and Bosshard, H. R. (1998) *Biochemistry 37*, 7539−7550.
23. Sang, B. C., and Barbosa, M. S. (1992) *Proc. Natl. Acad. Sci. U.S.A. 89*, 8063−8067.
24. Armstrong, D. J., and Roman, A. (1993) *Biochem. Biophys. Res. Commun. 192*, 1380−1387.
25. Kirk, W. R., Kurian, E., and Prendergast, F. G. (1996) *Biophys. J. 70*, 69−83.
26. Lima, L. M., and de Prat-Gay, G. (1997) *J. Biol. Chem. 272*, 19295−19303.
27. Howley, P. M., and Lowy, D. R. (2001) in *Fields Virology* (Knipe, D. M., and Howley, P. M., Eds.) pp 2197−2231, Lippincott, Williams & Wilkins, Philadelphia.
28. Imai, Y., Matsushima, Y., Sugimura, T., and Terada, M. (1991) *J. Virol. 65*, 4966−4972.
29. Patrick, D. R., Zhang, K., Defeo-Jones, D., Vuocolo, G. R., Maigetter, R. Z., Sardana, M. K., Oliff, A., and Heimbrook, D. C. (1992) *J. Biol. Chem. 267*, 6910−6915.
30. Brokaw, J. L., Yee, C. L., and Munger, K. (1994) *Virology 205*, 603−607.
31. Tourmadje, A., and Johnson, C., W. (1995) *J. Am. Chem. Soc. 117*, 7023−7024.
32. Weinreb, P. H., Zhen, W., Poon, A. W., Conway, A. K., and Lansbury, P. T. (1996) *Biochemistry 35*, 13709−13715.
33. Uversky, V. N., Gillespie, J. R., Millett, I. S., Khodyakova, A. V., Vasiliev, A. M., Chernovskaya, T. V., Vasilenko, R. N., Kozlovskaya, G. D., Dolgikh, D. A., Fink, A. L., Doniach, S., and Abramov, V. M. (1999) *Biochemistry 38*, 15009−15016.
34. Uversky, V. N., Gillespie, J. R., and Fink, A. L. (2000) *Proteins 41*, 415−427.

BI025579N